Colloid and Polymer Science
https://doi.org/10.1007/s00396-022-05043-4

ORIGINAL CONTRIBUTION

Morphological, rheological, and mechanical properties of PLA/TPU/nanoclay blends compatibilized with epoxy-based Joncryl chain extender

Yusuf Kahraman[1] · Burcu Özdemir[1] · Beril Eker Gümüş[2] · Mohammadreza Nofar[1]

Received: 2 May 2022 / Revised: 9 November 2022 / Accepted: 11 November 2022
© The Author(s), under exclusive licence to Springer-Verlag GmbH Germany, part of Springer Nature 2022

Abstract

This study investigates the synergistic effects of Cloisite 30B nanoclay and epoxy-based Joncryl chain extender on the morphological, rheological, and mechanical properties of PLA/TPU blends. Blends of PLA and 25 wt% TPU were melt compounded with nanoclay at various contents of 1, 3, and 5 wt% with and without 0.5 wt% Joncryl. Transmission and scanning electron microscopy analyses confirmed the interfacial localization of nanoclay. While the presence of nanoclay at the interface refined the droplet morphology, the incorporation of chain extender further decreased the TPU droplet size. Such interfacial localization of clay and its excessive dispersion within PLA as well as the refinement of droplets improved the melt viscoelastic properties of the blends specifically at low frequencies. The addition of chain extender also improved the impact strength and ductility of the blends, although the nanoclay incorporation suppressed these characteristics. The addition of nanoclay, however, enhanced the strength and modulus of the blend systems.

Keywords PLA · TPU · Blend · Nanoclay · Chain extender · Cloisite 30B · Joncryl

Introduction

Polylactide (PLA)-based compounds could nowadays be considered for many commodity and engineering applications. This is due to PLA's good mechanical, thermal, and physical properties although it also suffers from several drawbacks such as brittleness, low melt strength, and slow crystallization [1–8]. In order to improve the ductility, toughness, and melt properties of PLA, it is possible to blend PLA with various biopolymers [2, 4, 9–13] and synthetic non-compostable thermoplastics [10, 14–16]. So far, it has been confirmed that blending PLA with thermoplastic polyurethane (TPU), which possesses high toughness, biocompatibility, and durability, could be an effective way to improve the toughness and melt properties of PLA. However, PLA/TPU blends are immiscible systems; thus, physical properties of blends are highly dependent on their morphological features. While the competition between the droplet breakup and coalescence of dispersed phase defines the final morphology of PLA/TPU blends, it is also crucial to improve the phase compatibility and stabilize the morphology of the minor phase [17–19].

Chain extenders could act as compatibilizers by decreasing the interfacial tension between two phases, which could also stabilize the morphology of the secondary phase [20]. Our previous works revealed that the use of Joncryl ADR 4468 chain extender (CE) enhanced the interfacial compatibility between PLA and TPU, and caused improvements in the final morphological, rheological, and mechanical properties of corresponding blends. Moreover, it was also showed that TPU with ester-based soft segment had a better compatibility with PLA and hence the mechanical properties of the corresponding blends were improved more remarkably. It was confirmed that the strain at break and impact strength values of PLA/TPU blends (75 wt%/25 wt%) with only 0.5 wt% of CE were increased up to around 175% and 110 kJ/m^2, respectively [10, 21].

The incorporation of nanoparticles in PLA blends also stabilizes and refines the droplet morphology, which could

✉ Mohammadreza Nofar
nofar@itu.edu.tr

[1] Sustainable & Green Plastics Laboratory, Metallurgical & Materials Engineering Department, Faculty of Chemical and Metallurgical Engineering, Istanbul Technical University, Maslak, Istanbul 34469, Turkey

[2] Science and Technology Application and Research Center, Yıldız Technical University, Esenler, Istanbul 34220, Turkey

Published online: 29 November 2022

also prevent the use of compatibilizers [2, 19, 22]. In a polymer blend nanocomposite with droplet morphology, nanoparticles could localize at polymer phases or at the interface, and the latter case could prevent the coalescence of minor phase [23, 24]. Salehiyan et al. [25] compared the localization of various nanoparticles within PLA/PBAT blends and confirmed that C30B localizes at the interface of PLA/PBAT. Such interfacial localization prevents the droplet coalescence under shear flows [23]. Kilic et al. [26] investigated the compatibilization effect of triglycidylisobutyl polyhedral oligomeric silsesquioxane (TEpPOSS) on the properties of PLA/TPU blends. They revealed interfacial localization of TEpPOSS which refined the droplet sizes and enhanced the rheological properties. Oliaei et al. [27] showed that the interfacial localization of halloysite (HNT) clay converted the sea-island morphology of PLA/TPU blends to a semi-continuous structure and the addition of 6 wt% HNT increased the tensile strength and strain at break of blend nanocomposite. Kratochvíl and Kelnar [28] also confirmed that the incorporation of both C30B and HNT nanoclays reduced the droplet size of TPU within PLA matrix.

Studies have shown that the use of layered nanoclay offers series of advantages such as enhancements of mechanical properties together with improvements in barrier features [29]. The use of modified nanoclays could however cause the PLA's degradation during the melt processing, although the incorporation of chain extenders together with organoclays could be proposed as a breakthrough to compensate such molecular scission [30, 31]. Mirzadeh et al. [32] observed enhancements in mechanical and rheological properties of PLA/PBSA blends with the use of nanoclay and chain extender. They showed that the simultaneous incorporation of nanoclay and chain extender enhanced the viscoelastic properties of the blends while the interfacially localized nanoclay reduced the droplet size. Freitas et al. [33] also studied the simultaneous incorporation of the organoclays and chain extender on the properties of PLA/PBAT blends although the used nanoclay (Cloisite 20A) was not a compatible modified one to be properly dispersed with such polyester polymers.

In our recent studies [10, 21], it was showed that the incorporation of Joncryl ADR 4468 in PLA/TPU blends significantly refined the TPU droplets and caused significant improvements in rheological and mechanical properties specifically in blends at the weight ratio of 75/25 with 0.5 wt% CE. Tentative reaction mechanism of Joncryl with PLA and TPU was also evaluated in our previous studies. Joncryl's reactive sites interacted with end groups of PLA and TPU. Rheological analyses also revealed that Joncryl was more reactive with PLA. Therefore, compatibility between PLA and TPU improved due to the incorporation of Joncryl. In this study, PLA/TPU blends were prepared with different Cloisite 30B nanoclay contents (i.e., 1, 3, and 5 wt%) and with and without 0.5 wt% Joncryl CE. The effect of nanoclay content and the synergistic effect of nanoclay and chain extender on the resultant morphological, rheological, thermomechanical, and mechanical properties were then analyzed.

Experimental

Materials

A semicrystalline PLA grade (Ingeo 2500HP), with D-content of 0.5 mol%, was supplied from NatureWorks LLC. The glass transition (T_g) and the melting (T_m) temperatures were reported as around 60 and 175 °C, respectively. An ester-based TPU (Ravathane® 165 A85) was also supplied from Ravago Petrochemicals Production Inc. The molecular weight and shore hardness values were determined as 295 kg/mol and 85A, respectively [10]. The organo-modified nanoclay Cloisite 30B was supplied from Southern Clay Products Inc. Epoxy-based Joncryl ADR-4468 chain extender was also supplied by BASF. The molecular weight and high number average functionality of the chain extender were determined as 7.25 kg/mol and (fn > 4), respectively [20]. Throughout this study, Cloisite 30B nanoclay and Joncryl ADR-4468 chain extender are referred to as C30B and CE, respectively. The chemical structure of polymer components and CE is also illustrated in Fig. 1.

Blend preparation

2,3-Epoxypropyl methacrylate blends of PLA and 25 wt% TPU with varying C30B contents of 1, 3, and 5 wt% were melt blended with or without 0.5 wt% of CE. Blend components were dried overnight in a vacuum oven at 50 °C prior to the melt blending. A co-rotating twin screw extruder (Polmak, Turkey) having 18 mm diameter and L/D of 40 was used for melt blending at a rotation speed of 70 rpm. The barrel temperature profile was set at 170 °C-175 °C-180 °C-185 °C-190 °C (from the hopper to the die). The samples were coded with respect to the weight ratio of their constituents. For instance, blend nanocomposite containing 25 wt% TPU, 1 wt% of C30B, and 0.5 wt% CE is named as PLA/TPU/1C30B/CE. The test samples were prepared through compression molding at 190 °C by gradually increasing the pressure up to 1.5 tons for 5 min. The samples were taken out from the mold after being fast cooled with water circulation through the mold.

Morphological analysis

Scanning electron microscopy (SEM) images were obtained using a Zeiss EVO LS 10 in order to observe the morphological changes in blends. The samples were cryofractured with liquid nitrogen and their surfaces were coated with thin layer of Au–Pd prior to the analysis.

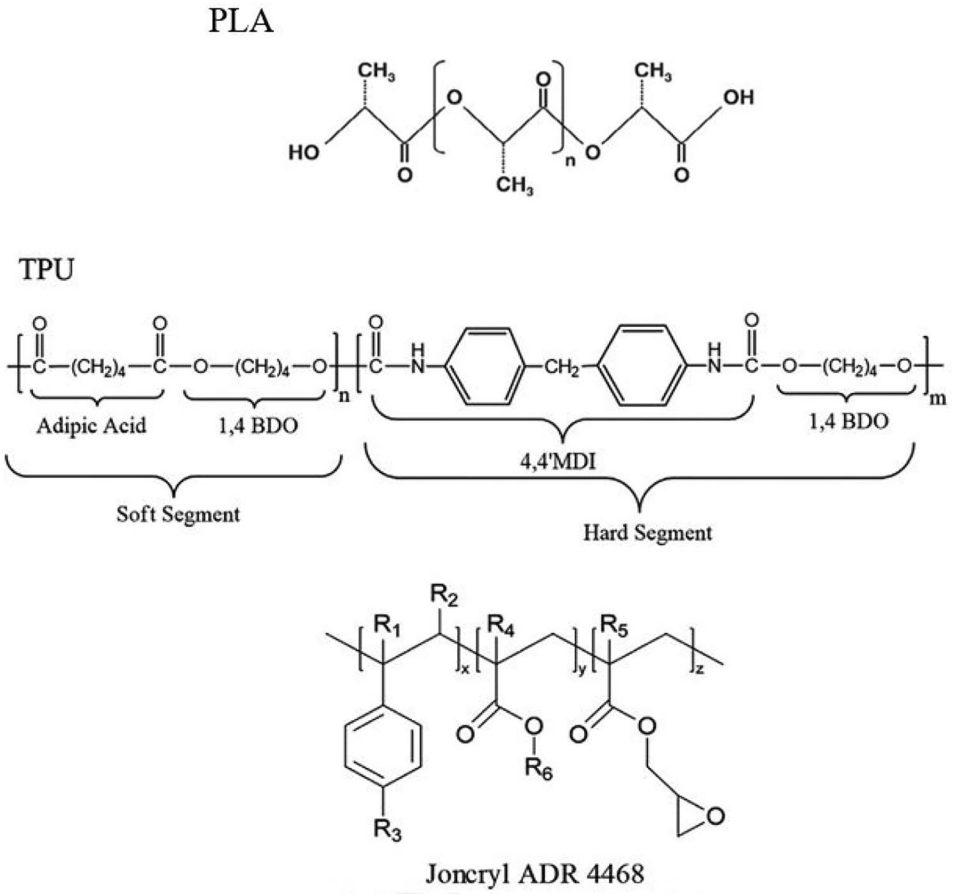

Fig. 1 Chemical structure of PLA, TPU, and Joncryl ADR 4468 chain extender [10, 21]

Transmission electron microscopy (TEM) images of nanocomposites with 3 wt% C30B were obtained using a G2 Spirit BioTWIN TEM (Tecnai) using a LaB 6 20–120 kV electron beam. Thin samples of 60–80 nm thickness were prepared using a microtome.

C30B dispersion and crystallization behavior of PLA were also determined by wide-angle X-ray diffractometer (WAXD) using a PANalytical, X'Pert PRO diffractometer (Cu-Kα radiation, 40 kV and 40 mA) at a scan rate of 0.015°/s over a range of $2\theta = 1–30°$.

Fourier transform infrared spectroscopy (FTIR) analysis was conducted in the mid-IR range (650–4000 cm^{-1}) using a Perkin Elmer Spectrum 100 spectrometer with an accessory of attenuated total reflectance (ATR). Sample measurements were conducted on dried grinded samples. Each spectrum was taken over 16 scans with a resolution of 2 cm^{-1}.

Rheological measurements

Small amplitude oscillatory shear (SAOS) rheological tests were performed at 190 °C using an MCR-301 rotational rheometer (Anton Paar) equipped with a parallel plate of 25 mm diameter with the gap set to 1 mm. Frequency sweep experiments were conducted from high to low frequencies (600 to 0.1 rad/s) using a strain amplitude of 0.01 under nitrogen atmosphere.

Dynamic mechanical analysis

Thermomechanical properties of the blends and nanocomposites were measured using a Perkin Elmer Dynamic Mechanical Analysis 8000 through temperature sweep experiments. The specimens were rectangular with 2 mm thickness, 50 mm length, and 10 mm width. The tests were conducted in single cantilever bending mode at an amplitude of 30 µm, with a frequency of 1 Hz, and a heating rate of 3 °C/min between 25 and 120 °C.

Mechanical properties

Tensile properties of the samples were analyzed using an Instron 8872 machine with the cross-head speed of 5 mm/min. Dog-bone samples were prepared with gage length of 20 mm and the thickness of 3 mm and width of 4 mm.

Izod impact tests of the samples were also conducted with Zwick 5105 impact device. Rectangular samples were prepared with 4 mm thickness, 80 mm length, and 10 mm width.

Results and discussion

Thermodynamics effects on the C30B localization in PLA/TPU blends

The thermodynamic equilibrium localization of fillers in polymer blends can be estimated by using interfacial tension values between polymers and polymer/nanoparticles using the Young's model (Eq. 1) [34]:

$$\omega = \frac{\gamma_{filler-polymerA} - \gamma_{filler-polymerB}}{\gamma_{polymerA-polymerB}} \quad (1)$$

where ω, $\gamma_{filler-polymerA}$, $\gamma_{filler-polymerB}$, and $\gamma_{polymerA-polymerB}$ are the wetting parameter, the interfacial tension between filler–polymer A, filler–polymer B, and polymer A-polymer B, respectively [35]. When $\omega < -1$, the filler locates only in polymer B; for $\omega > 1$, filler locates only in polymer A; and for $-1 < \omega < 1$, filler preferentially locates at the interface between two phases. The interfacial tension between filler–polymer and polymer–polymer could be estimated using the geometric mean equation (Eq. 2) [36]:

$$\gamma_{xy} = \gamma_x + \gamma_y - 2[\left(\gamma^d{}_x\gamma^d{}_y\right)^{\frac{1}{2}} + \left(\gamma^p{}_x\gamma^p{}_y\right)^{\frac{1}{2}}] \quad (2)$$

where γ_{xy} is the interfacial tension between components x and y, γ_x is the surface tension of material x,γ_y is the surface tension of material y, $\gamma^d{}_x$, $\gamma^d{}_y$ and $\gamma^p{}_x$, $\gamma^p{}_y$ are the dispersive and polar components of surface tension of the same materials, respectively.

To calculate the interfacial tension, the surface tensions of PLA, TPU, and C30B were calculated at 25 °C and extrapolated at 190 °C (i.e., the processing temperature) using corresponding thermal coefficients obtained from literature [23, 37]. The surface tension, including the polar and dispersive components of PLA, TPU, and C30B at 25 °C and 190 °C, and the interfacial tensions calculated by Eq. 2 are given in Table 1. In order to predict the localization of C30B in PLA/TPU blend using Eq. 1, wetting parameter ω is calculated as 4.97. Therefore, it can be estimated that the C30B thermodynamically prefers to be localized in the major phase.

WAXD and electron microscopy analyses of PLA/TPU blends

Figure 2A shows the WAXD patterns of C30B and PLA/TPU blend nanocomposites with different nanoclay contents (1, 3, and 5 wt%) between 2θ = 2–10°. The characteristic peak of neat C30B at 2θ = 4.73° corresponds to an interlayer d-spacing of 1.86 nm (Fig. 2a). The 2θ peaks of C30B in PLA/TPU/1C30B, PLA/TPU/3C30B, and PLA/TPU/5C30B blend nanocomposites shifted to lower values corresponding to higher d-spacing values of around 4.27, 3.91, and 3.40 nm, respectively. Such increase in d-spacing of C30B in blend nanocomposites is a result of intercalation of clay particles and a good level of exfoliation. The d-spacing decrease with clay content could also be due to the higher chance of agglomeration of nanoparticles at higher contents.

Figure 2b also shows the WAXD patterns of PLA and PLA/TPU blend nanocomposites with compatibilizer in the range 2θ = 10–30°. Main peaks of PLA α crystallites were appeared at 2θ = 13.8°, 16.7°, and 19.0°. The intensity of the peaks noticeably increased in blends specifically with the increase in C30B content up to 3 wt%. At 5 wt% C30B, however, the intensity of the main peak was reduced and broadened. Using the Scherrer equation [38] and considering the variations at main peak of 2θ = 16.7°, the PLA crystallite size in PLA, PLA/TPU, PLA/TPU/CE, PLA/TPU/1C30B/CE, PLA/TPU/3C30B/CE, and PLA/TPU/5C30B/CE were, respectively, estimated as 21.0, 26.2, 19.1, 23.4, 30.0, and 11.7 nm (the Scherrer constant, K, used in our calculations was 0.94). Such variations in the main peak of PLA α crystallites show that the increase in nanoclay content up to 3 wt% increases the size of the crystallites with higher closed packed structures. This is while in the blend with 5 wt% clay, the crystallites size reduces

Table 1 Surface tension parameters of PLA, TPU, and C30B at 25 and 190 °C as well as the calculated interfacial tensions at 190 °C

	Surface energies (mN/m)				Thermal coefficient	Interfacial tension (mN/m)	
	T (°C)	γ	γ^d	γ^p	$d\gamma/dT$	γ_{12} (190 °C)	
PLA [23]	25	50	37	13	−0.06 [37]	PLA/TPU	0.69
	190	40.1	28.90	10.15			
TPU [37]	25	41.69	30.36	11.33	−0.06 [37]	PLA/C30B	3.66
	190	31.79	23.71	8.85			
C30B [23]	25	35	22.4	12.6	−0.06 [23]	TPU/C30B	0.23
	190	25.1	16	8.9			

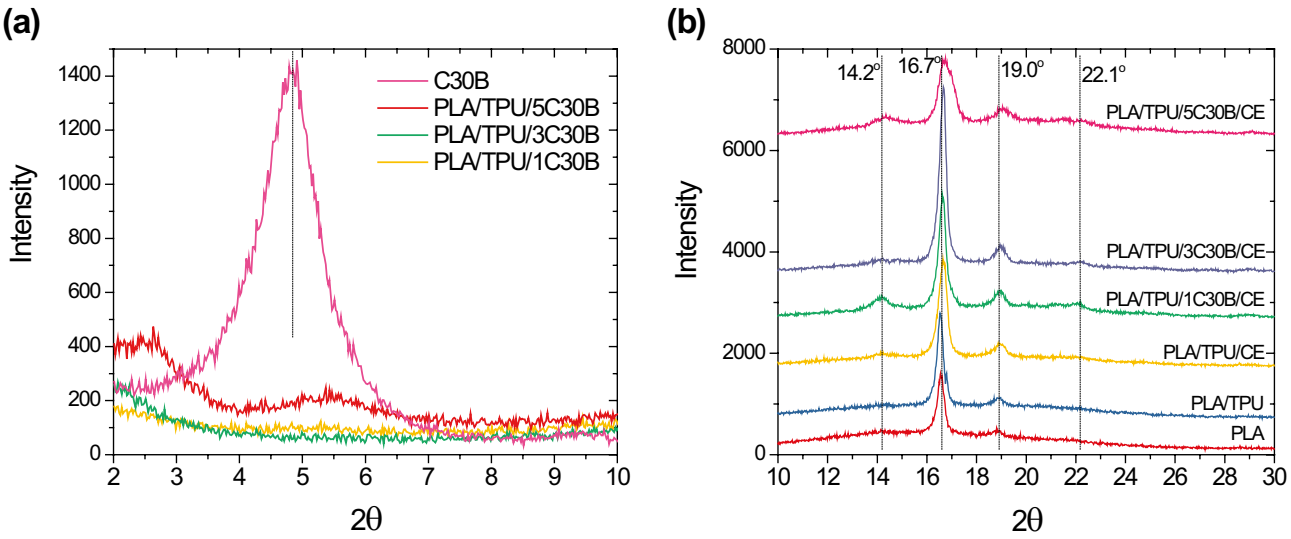

Fig. 2 WAXD results exhibiting **a** the C30B dispersion quality within PLA/TPU blend nanocomposites and **b** the crystallization behavior of PLA

dramatically with less closed packed structure as a results of increased crystal nucleation which could also hinder the crystal growth rate and perfection of the crystallites [39].

Figure 3 shows the TEM images of PLA/TPU/3C30B blend nanocomposite with and without CE. In PLA/TPU/C30B blend nanocomposites (Fig. 3a and a'), exfoliated C30B were mainly

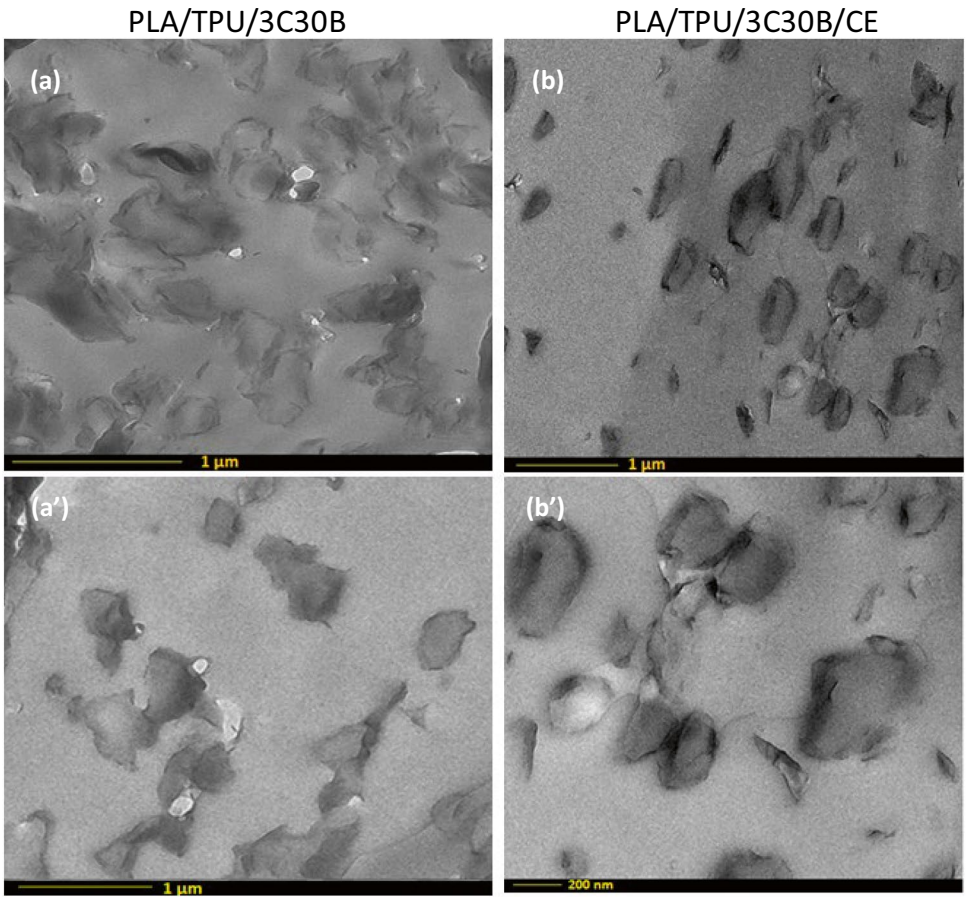

Fig. 3 TEM images of PLA/TPU/3C30B (**a**, **a'**) and PLA/TPU/3C30B/CE (**b**, **b'**)

found to be localized at the interphase of PLA and TPU while some excessive nanoclays also present in major or minor phases. Such kind of localization of nanoclays is opposed to thermodynamical calculations which could be related with extrapolation error or other kinetical parameters. In PLA/TPU/C30B/CE blend (Fig. 3b and b'), the droplet size of TPU phase was significantly reduced due the compatibilization effect of CE as well as the increased viscosity of PLA matrix (as a result of branching of PLA molecules). Such compatibilization effect and the matrix viscosity increase lead to further droplet breakup and hence finer minor phase. The clay localization was also similar to that in unmodified system and nanoclays were mainly observed at the interface of the compatibilized blend system while some excessive C30B also appeared in the major or minor phase. Such interfacial localization could also prevent the droplet coalescence during melt mixing, which could also contribute to the formation of finer TPU drops. On the other hand, the increase in matrix viscosity could also lead to a better nanoclay dispersion as a result of higher shear forces that could apply to exfoliate the layered particles.

Figure 4 shows the SEM images of PLA/TPU blend nanocomposites (0, 1, 3, and 5 wt% C30B) with and without CE. According to Fig. 4a–d, the incorporation of C30B resulted in finer TPU droplet morphology. As the amount of C30B increased, finer TPU droplets could be observed. Number averaged droplet sizes of TPUs in blends of neat PLA/TPU, PLA/TPU/1C30B, PLA/TPU/3C30B, and PLA/TPU/5C30B were measured as 5.2 ± 1.01, 2.12 ± 0.71, 1.44 ± 0.31, and 0.48 ± 0.33 μm, respectively. While in the case of compatibilized blends of PLA/TPU/CE, PLA/TPU/1C30B/CE, PLA/TPU/3C30B/CE, and PLA/TPU/5C30B/CE, average TPU droplet sizes were measured as 1.38 ± 0.59, 1.66 ± 0.44, 1.04 ± 0.27, and 0.42 ± 0.23 μm, respectively. This could be because of interfacially localized nanoclays, which could prevent the TPU droplet coalescence during the mixing [23]. According to this C30B localized at the interface provides decrease in droplet size. Clays act as shield and stabilize the morphology of blend. In such a scenario, interfacial localization of nanoclays immobilizes the interface and prevents the coalescence of droplets. In modified polymer nanocomposites (Fig. 4a'–d'), such droplet morphology refinement was even more significant and lead to the formation of much finer TPU droplets compared to their unmodified counterparts. This was due to the additional compatibilization effect of CE as well as the increased matrix viscosity (increased branching degree), which further caused the droplet breakup and refinement.

Rheological properties of blends

The complex viscosity (η^*) and storage modulus (G') values of neat PLA and PLA/TPU blend versus PLA/TPU blend nanocomposites with and without CE are shown in Fig. 5a–a' and b–b', respectively. In PLA/TPU/C30B blend nanocomposites without CE, low frequency upturn shifts in the complex viscosity and storage modulus reflect the shape relaxation behavior of the second phase (Fig. 4a–b). Localization of C30B at the interface and the decrease in TPU droplet size also play important roles on such upturns of viscoelastic properties. Moreover, the complex viscosity increased proportional to nanoclay content while the slope of the storage modulus decreased. Such an increase in complex viscosity could be related to stronger interaction of clay with polymer due to the enhanced interaction as a result of good exfoliation and distribution in polymer structure. The low frequency upturn was not significant in blend nanocomposite with 5 wt% of C30B compared to blend nanocomposites with 1 and 3 wt% of C30B. This could be due to inadequate effect of partially agglomerated C30B on viscoelastic properties at high contents. The increase in complex viscosity of compatibilized blend nanocomposites might be resulted from the refinement in droplet sizes, interface localization of nanoclays, and presence of excessive C30B in PLA matrix. Storage modulus of PLA/TPU/C30/CE blends were also increased at low frequency region while in the case of high amount of C30B loadings decrease in slope could be related with solid-like behavior due to the agglomeration.

FTIR analysis

Figure 6a–b shows the normalized FTIR spectra of PLA/TPU blends and blend nanocomposites without and with CE. The sharp peak around 1700 is related with >C==O stretching of TPU while peaks around 1160 belong to the C–O–C ester group of TPU. Moreover, the peaks at 2935 and 2850 cm^{-1} exist due to the vibration of $–CH_2$ groups which are characteristic for TPU. In the case of PLA/TPU/3C30B and PLA/TPU/5C30B, the localization of the nanoclays at the interface and restricted motion of polymer chains due to the agglomerated particles with increasing nanoclay content might prevent vibration of TPU molecules [40]. In Fig. 6a, the change in intensity of $–CH_2$ vibrations is related to altering droplet size of TPU and intercalation of C30B due to the increasing clay content that could affect the ordering of hard and soft segment domains. C30B supposed to show absorption peaks around 3644 and 3411 cm^{-1} due to the hydroxyl groups of silanol but due to the good exfoliation C30B no strong peak is detected. Addition of C30B decreased the carbonyl peak around 1700 cm^{-1} significantly both for blends with and without modification. Synergistic incorporation of C30B and CE also caused decrease in intensity of the peak due to the hydrogen bonding of carbonyl groups with reactive groups of C30B and CE. The change in peak intensities was observed due to the restriction of molecular vibrations and consuming of CE's reactive groups.

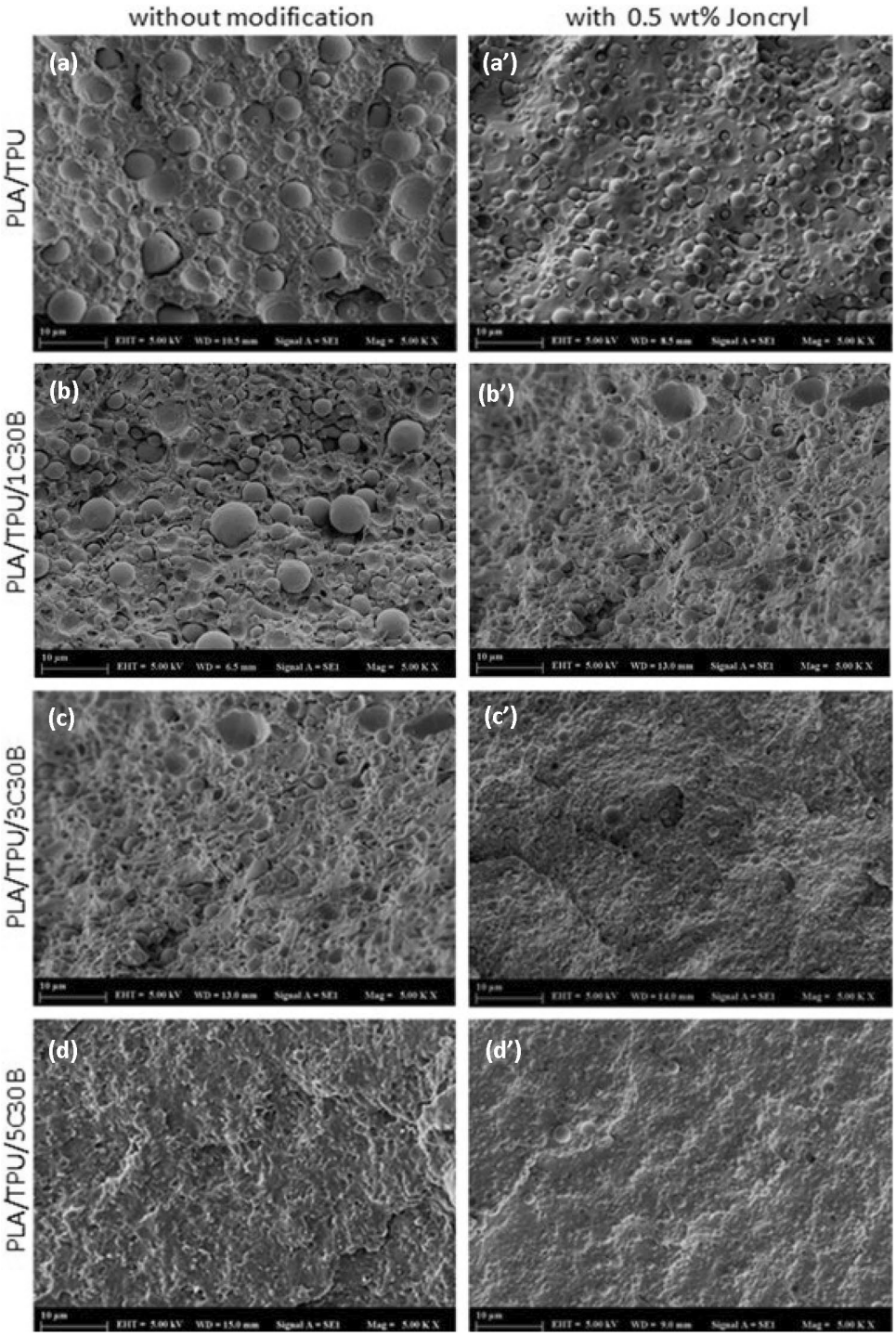

Fig. 4 SEM images of PLA/TPU, PLA/TPU/1C30B, PLA/TPU/3C30B, PLA/TPU/5C30B (**a**, **b**, **c**, **d**), PLA/TPU/CE, PLA/TPU/1C30B/CE, PLA/TPU/3C30B/CE, PLA/TPU/5C30B/CE (**a'**, **b'**, **c'**, **d'**) (the scale bar is 10 μm)

As it was observed from our previous study, the reaction between PLA and CE is more pronounced when compared with TPU. Since the CE is less reactive with TPU, no observable strong new peak was observed even if reactions occur between TPU and CE. Such kind of result was expected since a similar result was also obtained by Freitas et al. [10, 23].

Dynamic mechanical analysis

Figure 7 compares the storage modulus and loss factor (tan δ) as a function of temperature for blend systems. In all blends and blend nanocomposites, the drop of storage modulus below the glass transition of PLA is a result of having TPU with lower modulus than PLA. As it can be seen in Fig. 7a–a', sudden drop

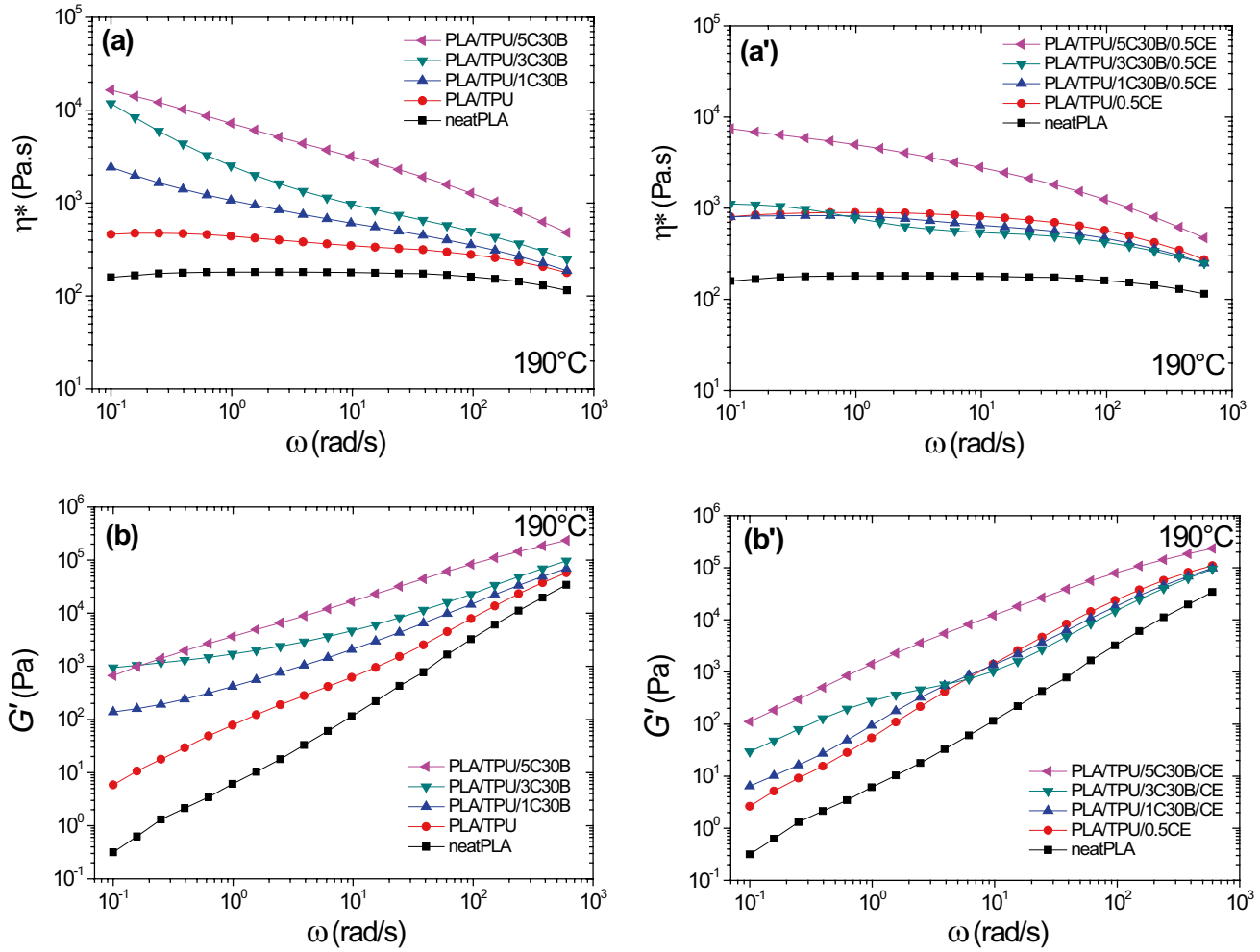

Fig. 5 Comparison of complex viscosities (**a**, **a'**) and storage modulus (**b**, **b'**) changes versus frequency of neat PLA, PLA/TPU and PLA/TPU/1C30B, PLA/TPU/3C30B, PLA/TPU/5C30B nanocomposites (**a**, **b**) with and without Joncryl (**a'**, **b'**)

in storage modulus is related to transition of glassy state to rubbery state at PLA's T_g. Moreover, increase in storage modulus of blend systems at around 100 °C is due to the cold crystallization of PLA. In Fig. 7b, intensity of the tan δ peak decreased with the addition of nanoclays due to the increased stiffness and restricted motion of polymer molecules. Additionally, in Fig. 7b', the tan

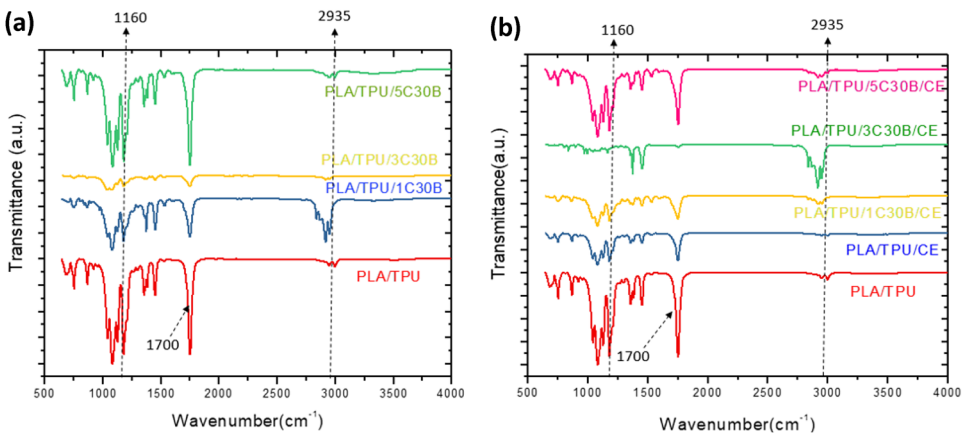

Fig. 6 FTIR spectra of PLA/TPU blend nanocomposites **a** without CE and **b** with CE

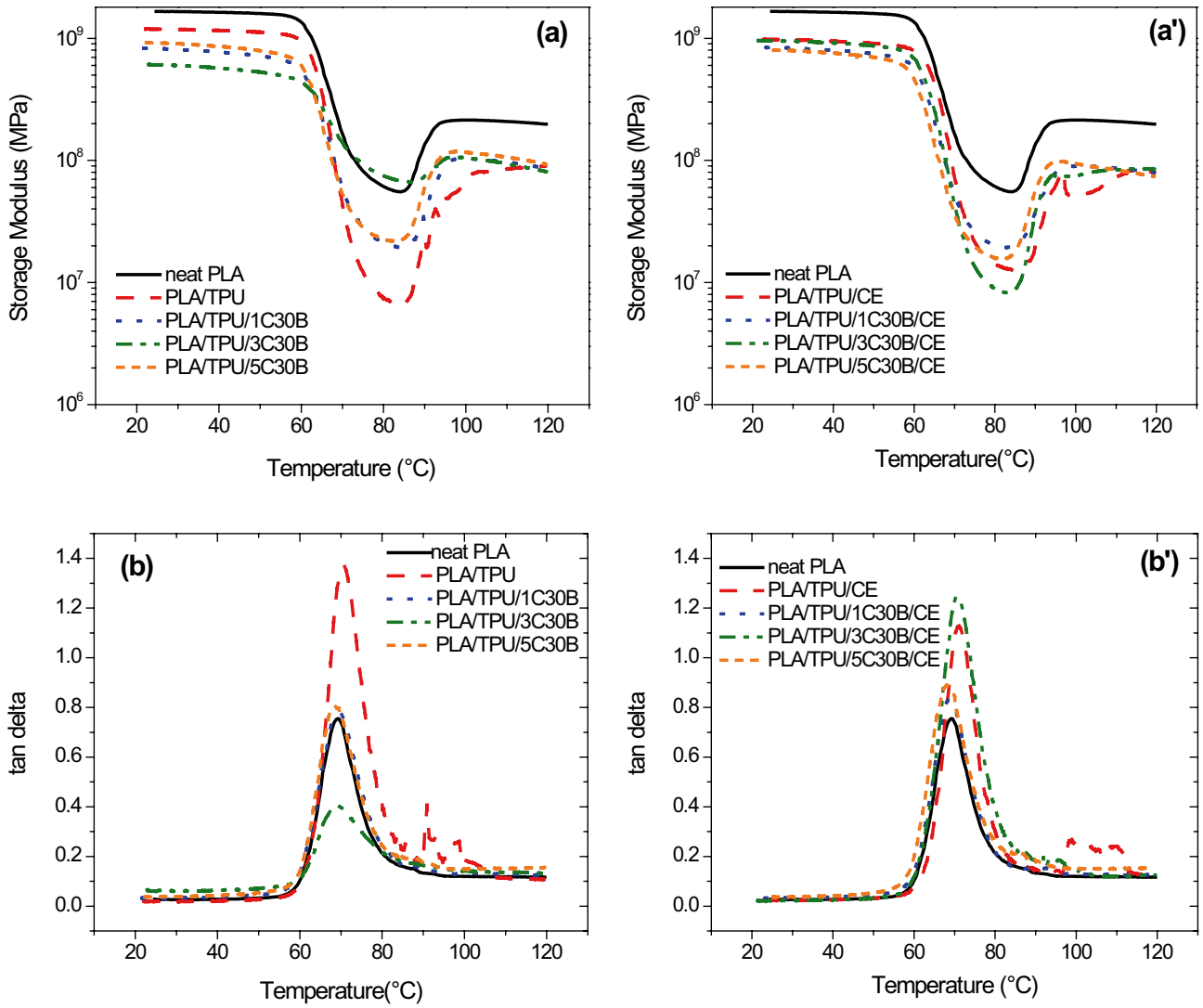

Fig. 7 Storage modulus (**a**, **a'**) and tan delta (**b**, **b'**) versus temperature graphs of neat PLA, PLA/TPU and PLA/TPU/1C30B, PLA/TPU/3C30B, PLA/TPU/5C30B nanocomposites without (**a**, **b**) and with (**a'**, **b'**) CE

δ peak of the compatibilized blend nanocomposites shifted to a higher temperature with the presence of CE which could also related to the restricted molecular movement due to the PLA molecules branching. However, such improvements in storage modulus and tan δ of compatibilized blend nanocomposites were not consistent with clay content increase due to the possible formation of clay aggregates at higher contents.

Mechanical properties

The notched Izod impact properties of the neat PLA and blend systems are presented in Fig. 8. Results showed that the incorporation of TPU increased the toughness of PLA to around 70 kJ/m^2, while addition of CE to PLA/TPU blend further increased the impact strength up to around 80 kJ/m^2 due to its compatibilization effect. However, the impact strength of PLA/TPU/C30B blend nanocomposites significantly decreased compared to that of PLA/TPU blend. Accordingly, as the amount of C30B increased, the impact strength of blend nanocomposites decreased. Moreover, PLA/TPU/5C30B blend nanocomposite revealed similar impact strength with neat PLA (20 kJ/m^2). In the case of modified PLA/TPU blend nanocomposite, impact strengths were comparable or slightly higher compared to counterparts without CE. However, the presence of C30B prevented the increase in impact strength of PLA/TPU blends comparable to those of PLA/TPU and PLA/TPU/CE. Such a result was expected since agglomerations with increasing clay content act as potential stress concentration in the blend and it causes premature failure of the material when exposed to impact forces.

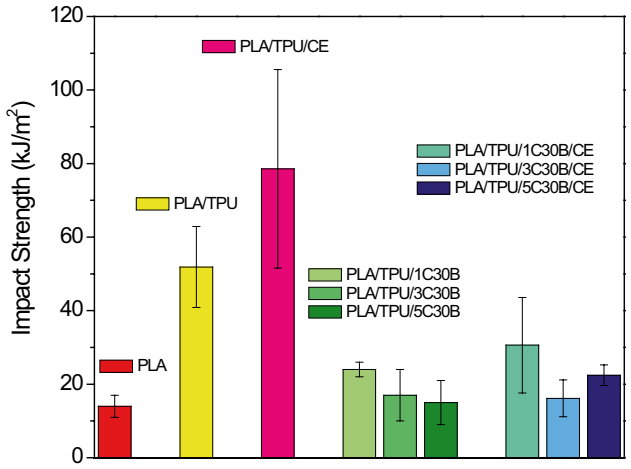

Fig. 8 Impact strength of neat PLA, PLA/TPU blend and PLA/TPU/C30B blend nanocomposites with/without CE

Tensile strength, modulus, and strain at break of the neat PLA and other blend systems are compared in Fig. 9. Tensile strength and modulus of PLA/TPU and PLA/TPU/CE decreased to around 30 MPa compared to neat PLA (~45 MPa). Moreover, tensile strength and modulus of the uncompatibilized PLA/TPU/C30B blend nanocomposites decreased compared to that of neat PLA/TPU blend. However, while tensile strength and modulus decreased, the strain at break values improved to some extent compared to that of PLA/TPU blend. Increase in ductility of blend nanocomposites could be related with fine droplet morphology in the blend. However, at 5 wt% of C30B content due to possible agglomeration, both the strength, modulus, and strain values further decreased compared to that of PLA/TPU blend. In compatibilized blend nanocomposites, both tensile strength and modulus improved compared to that of uncompatibilized blend systems. However, addition of C30B decreased the strain at break values possibly due to inherent rigidity of C30B. In PLA/TPU/1C30B/CE blend nanocomposite tensile strength reached up to around 45 MPa which was comparable to neat PLA, while the strain value increased to around 20% which was 4 times higher than that of PLA. Therefore, in order to reach high ductility and toughness values while not losing much of the strength and stiffness, the addition TPU with optimized CE and clay particles could be a breakthrough

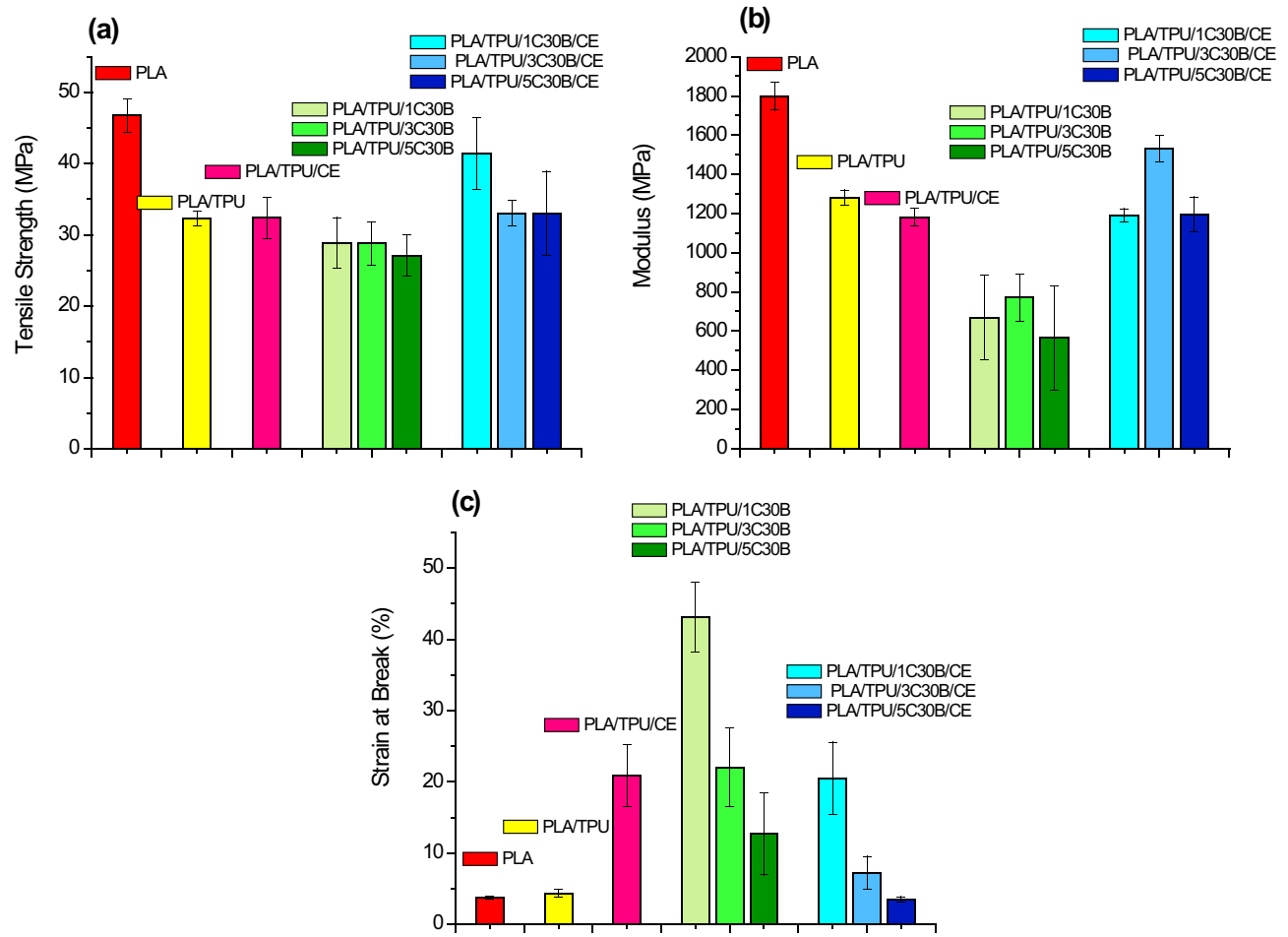

Fig. 9 Tensile strength (**a**), modulus (**b**), and strain at break (**c**) of the PLA/TPU nanocomposites with/without CE

to overcome some of PLA's inherent mechanical performance drawbacks.

Conclusion

Blend nanocomposites with and without Joncryl were prepared with different amount of C30B loadings in order to investigate the synergistic effects of CE and C30B on the morphological, rheological, and mechanical properties. In the case of PLA/TPU/3C30B, it was observed that C30B localized at the interface and some excessive C30B nanoclays also presented in minor TPU phase as opposed to thermodynamic estimations. Clay nanoparticles localized at the interface, which prevents the coalescence of droplets during melt mixing, refined the TPU droplets. The compatibilization effect of CE as well as increased viscosity of PLA matrix further contributed to the refinement of TPU droplets. As a result of such morphological refinement, the viscoelastic properties of the blends were differently influenced. Interfacial localization of nanoclays at the interface, decrease in TPU droplet sizes, and presence of excessive clay in matrix increased the storage modulus and complex viscosity of the blends. Also, blends with finer droplets exhibited enhanced tensile strength and modulus values when compared to unmodified counterparts. The addition of chain extender also improved the impact strength and ductility of the blends, although the nanoclay incorporation suppressed these characteristics. The addition of nanoclay, however, enhanced the strength and modulus of the blend systems.

Acknowledgements The authors would like to acknowledge the supports by Turkish Academy of Sciences (TÜBA)—Outstanding Young Scientists Award (GEBİP). We also thank Ravago Petrochemicals Production Inc. and Dr. Yakup Ulcer for kindly suppling TPU samples. We would also like to sincerely thank Prof. Dr. Gürbüz Güneş, Asst. Professor Omer Yunus Gumus, Dr. Aylin Bekem, Dr. Yonca Alkan, and Expert Zekeriya Yasar Comert for providing the lab space for sample processing and characterization.

Data availability Data not available/data will be made available on request.

Declarations

Competing interests The authors declare no competing interests.

References

1. Kijchavengkul T, Auras R (2008) Compostability of polymers. Polym Int 57(6):793–804. https://doi.org/10.1002/pi.2420
2. Nofar M, Sacligil D, Carreau PJ, Kamal MR, Heuzey MC (2019) Poly (lactic acid) blends: processing, properties and applications. Int J Biol Macromol 125:307–360. https://doi.org/10.1016/j.ijbiomac.2018.12.002
3. Hamad K, Kaseem M, Yang HW, Deri F, Ko YG (2015) Properties and medical applications of polylactic acid: a review. Express Polym Lett 9(5):435–455. https://doi.org/10.3144/expresspolymlett.2015.42
4. Nofar M (2021) Multiphase polylactide blends: toward a sustainable and green environment. Elsevier. eBook ISBN: 9780128241516
5. Garlotta D (2001) A literature review of poly(lactic acid). J Polym Environ 9(2):63–84. https://doi.org/10.1023/A:1020200822435
6. Ikada Y, Tsuji H (2000) Biodegradable polyesters for medical and ecological applications. Macromol Rapid Commun 21(3):1177–2132. https://doi.org/10.1002/(SICI)1521-3927(20000201)21:3%3c117::AID-MARC117%3e3.0.CO;2-X
7. Saeidlou S, Huneault MA, Li H, Park CB (2012) Poly(lactic acid) crystallization. Prog Polym Sci 37(12):1657–1677. https://doi.org/10.1016/j.progpolymsci.2012.07.005
8. Nofar M, Salehiyan R, Ray SS (2019) Rheology of poly(lactic acid) – based systems. Polym Rev 59(3):465–509. https://doi.org/10.1080/15583724.2019.1572185
9. Nofar M, Salehiyan R, Ciftci U, Jalali A, Durmuş A (2020) Ductility improvements of PLA-based binary and ternary blends with controlled morphology using PBAT, PBSA, and nanoclay. Compos B Eng 182:107661. https://doi.org/10.1016/j.compositesb.2019.10766
10. Kahraman Y, Özdemir B, Kılıç V, Goksu YA, Nofar M (2021) Super toughened and highly ductile PLA/TPU blend systems by in situ reactive interfacial compatibilization using multifunctional epoxy-based chain extender. J Appl Polym Sci 138(20):50457. https://doi.org/10.1002/app.50457
11. Salehiyan R, Yussuf AA, Hanani NF, Hassan A, Akbari A (2015) Polylactic acid/polycaprolactone nanocomposite: influence of montmorillonite and impact modifier on mechanical, thermal, and morphological properties. J Elastomers Plast 47(1):69–87. https://doi.org/10.1177/0095244313489906
12. Ojijo V, Sinha Ray S, Sadiku R (2013) Toughening of biodegradable polylactide/poly(butylene succinate-co-adipate) blends via in situ reactive compatibilization. ACS Appl Mater Interfaces 5(10):4266–4276. https://doi.org/10.1021/am400482f
13. Nofar M, Oguz H, Ovalı D (2019) Effects of the matrix crystallinity, dispersed phase, and processing type on the morphological, thermal, and mechanical properties of polylactide-based binary blends with poly[(butylene adipate)-co-terephthalate] andpoly[(butylene succinate)-co-adipate]. J Appl Polym Sci 136(23):47636–47647. https://doi.org/10.1002/app.47636
14. Yu R, Zhang L, Feng Y, Zhang R, Zhu J (2014) Improvement in toughness of polylactide by melt blending with bio-based poly(ester) urethane. Chin J Polym Sci 32(8):1099–1110. https://doi.org/10.1007/s10118-014-1487-9
15. Veenstra H, Van Dam J, Posthuma de Boer A (2000) On the coarsening of co-continuous morphologies in polymer blends: effect of interfacial tension, viscosity and physical cross-links. Polymer 41(8):3037–3045. https://doi.org/10.1016/S0032-3861(99)00455-3
16. Jašo V, Cvetinov M, Rakić S, Petrović ZS (2014) Bio-plastics and elastomers from polylactic acid/thermoplastic polyurethane blends. J Appl Polym Sci 131(22). https://doi.org/10.1002/app.41104
17. Li H, Sundararaj U (2009) Morphology development of polymer blends in extruder: the effects of compatibilization and rotation rate. Macromol Chem Phys 210(10):852–863. https://doi.org/10.1002/macp.200800543
18. Chen H-L, Li L-J, Lin T-L (1998) Formation of segregation morphology in crystalline/amorphous polymer blends: molecular weight effect. Macromolecules 31(7):2255–2264. https://doi.org/10.1021/ma9715740
19. Nofar M, Salehiyan R, Ray SS (2021) Influence of nanoparticles and their selective localization on the structure and properties

of polylactide-based blend nanocomposites. Compos B Eng 215:108845. https://doi.org/10.1016/j.compositesb.2021.108845
20. Standau T, Nofar M, Dörr D, Ruckdäschel H, Altstädt V (2021) A review on multifunctional epoxy-based Joncryl (R) ADR chain extended thermoplastics. Polym Rev. https://doi.org/10.1080/15583724.2021.1918710
21. Kahraman Y, Alkan Goksu Y, Özdemir B, Eker Gümüş B, Nofar M (2022) Composition design of PLA/TPU emulsion blends compatibilized with multifunctional epoxy-based chain extender to tackle high impact resistant ductile structures. J Appl Polym Sci 139(12):51833. https://doi.org/10.1002/app.51833
22. Sarul D, Arslan D, Vatansever E, Kahraman Y, Durmus A, Salehiyan R, Nofar M (2022) Effect of mixing strategy on the structure-properties of the PLA/PBAT blends incorporated with CNC. J Renew Mater 10(1):149–164. https://doi.org/10.32604/jrm.2022.017003
23. Nofar M, Heuzey M-C, Carreau PJ, Kamal MR (2016) Effects of nanoclay and its localization on the morphology stabilization of PLA/PBAT blends under shear flow. Polymer 98:353–364. https://doi.org/10.1016/j.polymer.2016.06.044
24. Mohammadi M, Heuzey M-C, Carreau PJ, Taguet A (2021) Interfacial localization of CNCs in PLA/PBAT blends and its effect on rheological, thermal, and mechanical properties. Polymer 233:124229. https://doi.org/10.1016/j.polymer.2021.124229
25. Salehiyan R, Nofar M, Malkappa K, Ray SS (2020) Effect of nanofillers characteristics and their selective localization on morphology development and rheological properties of melt-processed polylactide/poly(butylene adipate-co-terephthalate) blend composites. Polym Eng Sci 60(11):2749–2760. https://doi.org/10.1002/pen.25505
26. Kilic NT, Can BN, Kodal M, Özkoç G (2021) Reactive compatibilization of biodegradable PLA/TPU blends via hybrid nanoparticle. Prog Rubber Plast Recycl Technol 37(4):301–326. https://doi.org/10.1177/14777606211019423
27. Oliaei E, Kaffashi B, Davoodi S (2016) Investigation of structure and mechanical properties of toughened poly(l-lactide)/thermoplastic poly(ester urethane) blends. J Appl Polym Sci 133(15). https://doi.org/10.1002/app.43104
28. Kratochvíl J, Kelnar I (2017) Non-isothermal kinetics of cold crystallization in multicomponent PLA/thermoplastic polyurethane/nanofiller system. J Therm Anal Calorim 130(2):1043–1052. https://doi.org/10.1007/s10973-017-6417-y
29. Guo F, Aryana S, Han Y, Jiao Y (2018) A review of the synthesis and applications of polymer–nanoclay composites. Appl Sci 8(9):1696. https://doi.org/10.3390/app8091696
30. Najafi N, Heuzey MC, Carreau PJ, Wood-Adams PM (2012) Control of thermal degradation of polylactide (PLA)-clay nanocomposites using chain extenders. Polym Degrad Stab 97(4):554–565. https://doi.org/10.1016/j.polymdegradstab.2012.01.016
31. Najafi N, Heuzey MC, Carreau PJ (2012) Polylactide (PLA)-clay nanocomposites prepared by melt compounding in the presence of a chain extender. Compos Sci Technol 72(5):608–615. https://doi.org/10.1016/j.compscitech.2012.01.005
32. Mirzadeh A, Ghasemi H, Mahrous F, Kamal MR (2015) Reactive extrusion effects on rheological and mechanical properties of poly(lactic acid)/poly[(butylene succinate)-co-adipate]/epoxy chain extender blends and clay nanocomposites. J Appl Polym Sci 132(48). https://doi.org/10.1002/app.42664
33. Freitas ALPDL, Tonini Filho LR, Calvão PS, de Souza AMC (2017) Effect of montmorillonite and chain extender on rheological, morphological and biodegradation behavior of PLA/PBAT blends. Polym Testing 62:189–195. https://doi.org/10.1016/j.polymertesting.2017.06.030
34. Young T (1805) An essay on the cohesion of fluids. Philos Trans R Soc Lond 95:65–87. https://doi.org/10.1098/rstl.1805.0005
35. Fenouillot F, Cassagnau P, Majesté JC (2009) Uneven distribution of nanoparticles in immiscible fluids: morphology development in polymer blends. Polymer 50:1333–1350. https://doi.org/10.1016/j.polymer.2008.12.029
36. Kaelble DH (1971) Physical chemistry of adhesion; Wiley-Interscience; New York ISBN: 0471454117 9780471454113
37. Buys YF, Mawardi MA, Anuar H (2017) Selective localization of multi-walled CNT in polylactic acid/thermoplastic polyurethane blends and its effect on mechanical properties. Current Nanomaterials 2(2):84–89. https://doi.org/10.2174/2405461503666180226122550
38. Scherrer P (1918) Nachrichten von der Gesellschaft der Wissenschaften zu Göttingen, Mathematisch-Physikalische Klasse. 2:98–100
39. Nofar M, Zhu W, Park CB (2012) Effect of dissolved CO2 on the crystallization behavior of linear and branched PLA. Polymer 53(15):3341–3353. https://doi.org/10.1016/j.polymer.2012.04.054
40. Bordes P, Pollet E, Avérous L (2009) Nano-biocomposites: biodegradable polyester/nanoclay systems. Prog Polym Sci 34(2):125–155. https://doi.org/10.1016/j.polymertesting.2017.06.030

Publisher's Note Springer Nature remains neutral with regard to jurisdictional claims in published maps and institutional affiliations.

Springer Nature or its licensor (e.g. a society or other partner) holds exclusive rights to this article under a publishing agreement with the author(s) or other rightsholder(s); author self-archiving of the accepted manuscript version of this article is solely governed by the terms of such publishing agreement and applicable law.